Liquid Density and Bubble Pressure Measurements for the Propylene + 2-Propanol System

Paolo Stringari,[†] Giancarlo Scalabrin,*[,†] Dominique Richon,[‡] and Christophe Coquelet[‡]

Dipartimento di Fisica Tecnica, Università di Padova, via Venezia 1, I-35131 Padova, Italy, and Mines Paris Paris Tech, CEP/TEP, CNRS FRE 2861, 35, Rue Saint Honoré, 77305 Fontainebleau, France

Bubble pressures and liquid densities for the propylene (1) + 2-propanol (2) mixture have been determined at (300, 325, and 350) K and x_1 close to 0.20, 0.52, and 0.65 using a vibrating tube densimeter. Liquid densities have been measured from bubble pressures up to 10 MPa and correlated with a multilayer feedforward neural network. The composition dependence of the excess molar volume has been evaluated in the temperature and pressure range of the experimental data. Bubble pressures have been compared with a multilayer feedforward neural network function regressed on the available literature data showing a good consistency between the two. The multilayer feedforward neural network correlations for liquid density and bubble pressure have been used to generate the saturated liquid density surface in the whole temperature range and for compositions including the pure components. Excess molar volumes and bubble pressure predictions obtained by the neural network models have been compared with those from a Peng–Robinson equation of state with Wong−Sandler mixing rules to show the consistent behavior in the regions where data are lacking.

1. Introduction

The process industries, such as in particular the chemical ones, use a relevant fraction of their energy consumption for the separation processes of fluid mixtures. Apart from the conventional industrial separation processes, there is a rising need toward studying alternative methods compatible with the requirements of sustainable development, environmental impact, and energy saving.

The limited knowledge of the thermodynamics of systems particularly complex, such as for instance the polar and associating mixtures, hinders the development of analysis and optimization studies addressed to both the overall effectiveness and the energetic consumption.

In recent times, the separation processes of oxychemicals from aqueous solutions has received increasing consideration. The authors have previously considered an exemplifying system suitable for the development of an analyzing method for the present purpose which is 2-propanol + water + propylene.[1] In general, the kind of data simultaneously needed are basically coexistence, density, and calorimetric data. In this context, a well-known lack of experimental data hinders pursuing of the scope so that the data of interest have to be expressly measured.

In the present work, one of the binary mixtures composing the cited ternary system is studied, i.e., the propylene + 2-propanol one.

The literature presents a number of experimental works about this mixture which in particular are: vapor–liquid equilibria at constant temperature in a range from (333.1 to 373.1) K in Zabaloy et al.;[2] vapor pressure for diluted 2-propanol mixtures from (293.15 to 333.15) K in Guzechak et al.;[3] bubble pressures at 298.15 K and excess enthalpies at 333.1 K and 3.1 MPa in Horstmann et al.[4]

For the density and bubble pressure measurements a "synthetic open circuit method" taking advantage of a vibrating tube densimeter (VTD) was used, allowing to quickly get efficient density data; in fact, this is one of the most popular measuring methods in the literature. A previous study concerning the determination of single phase densities and bubble pressures was done using the same technique for the carbon dioxide + 2-propanol system.[5]

The obtained liquid density and bubble pressure values have been correlated using two multilayer feedforward neural network (MLFN) functions.

2. Experimental

2.1. Chemicals. The 2-propanol (molar mass = 60.096 kg·kmol^{-1}, CAS Number 67-63-0) is from Sigma-Aldrich with a GC certified purity higher than 99.8 %. The propylene (molar mass = 42.08 kg·kmol^{-1}, CAS Number 115-07-1) is from Air–Liquide with a certified purity higher than 99.99 vol %.

2.2. Apparatus. A detailed description of the apparatus is given in ref 6, and its schematic layout is presented in Figure 1. The apparatus employs a vibrating tube made of stainless steel (Anton Paar, model DMA 512). The period of vibration τ is recorded by means of a data acquisition unit (Hewlett-Packard, model 53131A). The temperature of the vibrating tube is controlled by a regulated liquid bath (Lauda, model RE206) with stability within ± 0.01 K. The temperature of the remaining parts of the circuit is regulated by a liquid bath (Bioblock, model Variosat P1C50P as the cooling source, electric resistor managed by a PID regulator West model 6100 as the heating source). Temperatures are measured with two Pt 100 probes connected to a data acquisition unit (Hewlett-Packard, model 34970A). The probes have been calibrated in the (288 to 433) K range against a 25 Ω reference thermometer (Tinsley Precision

* To whom correspondence should be addressed. Tel.: +39 049 827 6875. Fax: +39 049 927 6896. E-mail: gscala@unipd.it.
[†] Università di Padova.
[‡] Mines Paris Paris Tech.

10.1021/je800017j CCC: $40.75
Published on Web 03/27/2008

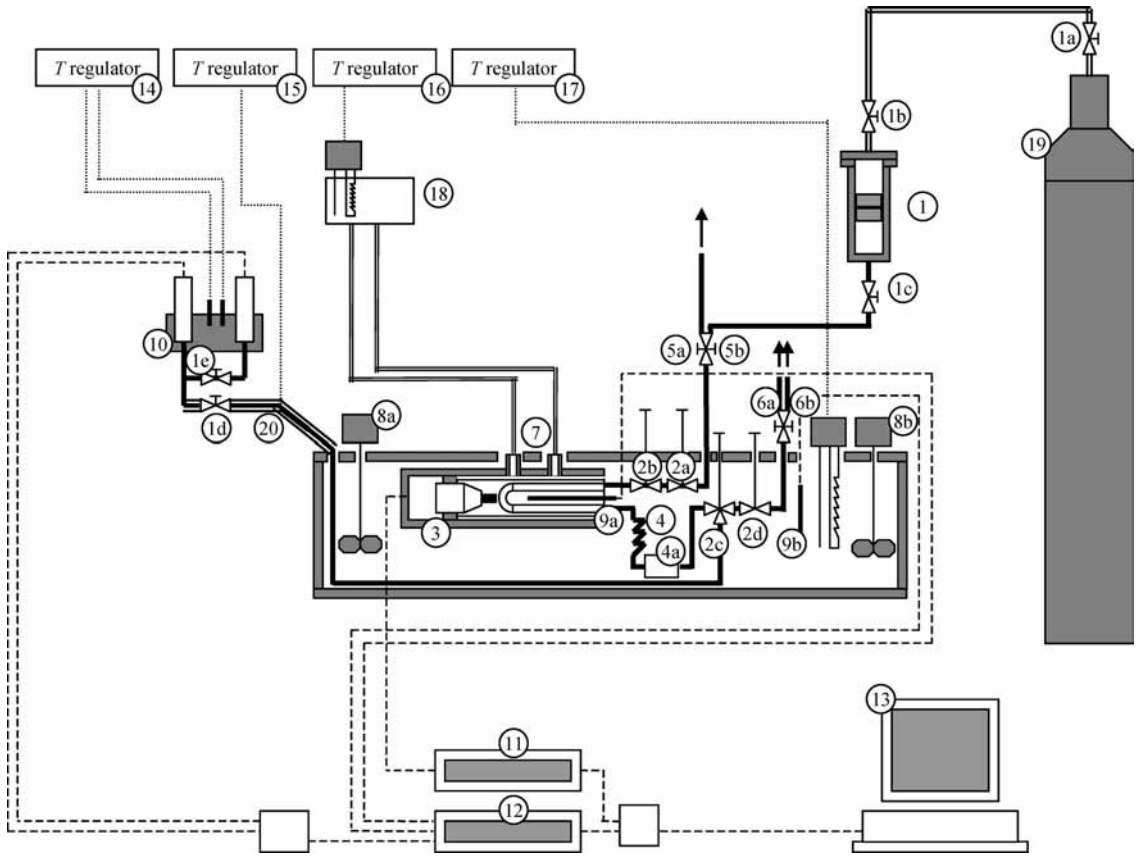

Figure 1. Flow diagram of the equipment: 1, loading cell; 1a−1e, shut-off valves; 2a and 2b, regulating and shut-off inlet valves; 2c and 2d, regulating and shut-off outlet valves; 3, densimeter; 4, heat exchanger; 4a, bursting disk; 5a, 5b, and 6a, 6b, double valves; 7, inlet and outlet for the VTD temperature regulation; 8a and 8b, mixers; 9a and 9b, Pt 100 probes; 10, pressure transducers maintained at constant temperature; 11, data acquisition unit; 12, data acquisition unit; 13, data acquisition supervising; 14, temperature regulator of the pressure transducers; 15, temperature regulator of the thermostatted tube (20); 16, temperature regulator of the liquid bath (18); 17, temperature regulator of the main liquid bath; 18, liquid bath; 19, nitrogen bomb; 20, thermostatted tube.

Instrument) certified by Laboratoire National d'Essais (Paris, France). Pressure is measured using two pressure transducers (Druck, model PTX611) of two complementary ranges: (0 to 0.5) MPa and (0.5 to 8.0) MPa. These sensors were calibrated against a dead weight pressure balance (Desgranges & Huot, model 5202S) in the (0.3 to 10.6) MPa range. The vacuum was achieved by means of a vacuum pump (AEG, model LN38066008). Real time (τ, T, P) data are recorded every 3 s by a computer linked to both the HP units. Synthetic mixtures have been prepared gravimetrically under a vacuum according to the procedures presented in ref 7. An analytical balance (Sartorius AG, Göttingen, model CC3000) was used to get accurate mass values. Viton 70 Shore O-rings have been used as seals for the piston in the loading cell.

2.3. Experimental Procedure. The description of the experimental procedure refers to the schematic layout of the equipment presented in Figure 1. The synthetic mixture is gravimetrically prepared in the loading cell (1) under vacuum, according to the procedure discussed in ref 7. The loading cell is connected to the circuit by means of the valve 1c and to a high-pressure nitrogen bomb by the valves 1a and 1b. Before starting the measurement, the VTD liquid bath (18) is programmed at the measurement temperature, while the main bath is programmed at a temperature slightly higher, (0.5–1) K, to obtain the first vaporization inside the VTD instead of in the other parts of the circuit (for details, see ref 6). The whole circuit was evacuated connecting the vacuum pump to the valve 5a, while valves from 2a to 2d and 5b are open and valves 1c, 6a, and 6b are closed. The period of vibration at the lowest accessible pressure, obtained with the vacuum pump, and at the measurement temperature is measured. To carry out density measurements in the liquid phase, the pressure in the loading cell is increased to values higher than the bubble pressure of the mixture to ensure the homogenization inside the cell. After the measurement of the vibration period at vacuum conditions, the vacuum pump is disconnected closing the valve 5a, and the fluid is loaded from the loading cell to the apparatus through the valve 1c. The movement of the piston inside the cell ensures the homogeneity of the mixture in the apparatus maintaining the mixture pressure constant during the loading of the circuit. If the loading pressure is higher than 0.5 MPa, the valve 1e has to be closed during this procedure to avoid damage of the low-pressure transducer. The circuit is partially purged, opening the valve 6a or 6b, and a new mixture is introduced in the circuit from the loading cell. It is assumed that the liquid inside the VTD is representative of the fluid inside the loading cell when the measured period of vibration remains constant and is not dependent on further purging. The pressure in the circuit is increased, opening the valve 1a up to the highest measurement pressure (about 10 MPa in this work). A suitable opening of the valve 2d is then selected to ensure that the pressure inside the circuit decreases continuously with a controlled rate not higher than 0.005 MPa·s^{-1}. Under these conditions, the fluid inside the apparatus is assumed in mechanical equilibrium. The liquid phase is studied from the chosen upper pressure down to the bubble point, which is determined through the drastic change in the $P \div \tau$ behavior going from the single phase to the coexistence region as described in ref 6. During this process,

Table 1. Experimental Liquid Density Data for the Propylene (1) + 2-Propanol (2) Mixture

$x_1 = 0.2011$

$T = 300.14$ K		$T = 325.09$ K		$T = 350.18$ K	
P/PMa	ρ/kg·m^{-3}	P/PMa	ρ/kg·m^{-3}	P/PMa	ρ/kg·m^{-3}
0.5294	731.63	0.8109	703.07	1.6395	677.13
1.0513	732.17	1.2189	703.59	2.0700	677.93
1.4836	732.72	1.6087	704.14	2.4462	678.64
1.9544	733.24	2.0018	704.70	2.9243	679.50
2.3840	733.72	2.3837	705.30	3.2714	680.17
2.7986	734.18	2.8276	705.86	3.6753	680.86
3.2731	734.68	3.1592	706.38	4.0584	681.60
3.7402	735.18	3.7079	707.07	4.4468	682.32
4.1863	735.68	4.1236	707.68	4.7913	682.93
4.7286	736.23	4.5285	708.19	5.1719	683.60
5.2356	736.78	4.9253	708.73	5.5574	684.26
5.7673	737.30	5.3707	709.32	6.0020	684.96
6.2747	737.83	5.8835	709.98	6.4302	685.69
6.8325	738.41	6.3362	710.58	7.0712	686.73
7.2915	738.89	6.7884	711.17	7.5705	687.62
7.8118	739.42	7.3466	711.90	7.9441	688.25
8.2966	739.90	7.8793	712.57	8.3868	688.92
8.8103	740.41	8.3925	713.18	8.8268	689.60
9.3377	740.91	8.9852	713.89	9.2790	690.38
9.8864	741.45	9.5877	714.65	9.7796	691.08

$x_1 = 0.5201$

$T = 300.11$ K		$T = 325.05$ K		$T = 350.12$ K	
P/PMa	ρ/kg·m^{-3}	P/PMa	ρ/kg·m^{-3}	P/PMa	ρ/kg·m^{-3}
0.9667	644.49	1.6131	613.41	2.3323	576.59
1.3733	645.21	1.9777	614.26	2.7314	577.92
1.8356	645.98	2.3590	615.15	2.9924	578.85
2.3409	646.83	2.7172	615.98	3.2180	579.68
2.8124	647.62	3.1678	616.93	3.5061	580.58
3.3301	648.49	3.5061	617.74	3.7656	581.46
3.8175	649.27	3.8888	618.59	4.2255	582.95
4.3861	650.18	4.3216	619.52	4.5506	583.87
4.8737	650.95	4.6767	620.29	4.8244	584.73
5.3752	651.72	5.0614	621.12	5.1037	585.64
5.8888	652.52	5.4718	621.94	5.3993	586.54
6.4420	653.35	5.8801	622.78	5.7155	587.44
6.9428	654.09	6.2936	623.65	5.9995	588.29
7.4982	654.90	6.7043	624.42	6.3039	589.18
8.1047	655.77	7.1717	625.34	6.6328	590.10
8.6718	656.58	7.5974	626.18	6.9755	591.05
9.2267	657.35	8.0375	627.02	7.2800	591.94
9.7870	658.16	8.5565	628.02	7.6413	592.87
		9.0781	628.97	7.9635	593.76
		9.6313	629.98	8.3120	594.68
				8.7624	595.82
				9.2110	596.88
				9.6229	597.92

$x_1 = 0.6478$

$T = 300.12$ K		$T = 325.13$ K		$T = 350.18$ K	
P/PMa	ρ/kg·m^{-3}	P/PMa	ρ/kg·m^{-3}	P/PMa	ρ/kg·m^{-3}
1.0685	608.06	1.7475	573.29	2.6890	531.01
1.4865	608.93	2.1518	574.52	3.1263	533.02
1.7406	609.48	2.6075	575.84	3.6862	535.68
2.1238	610.19	3.0221	577.00	3.9143	536.74
2.6200	611.17	3.4227	578.16	4.2032	537.97
2.9868	611.92	3.8263	579.23	4.4846	539.15
3.4953	612.85	4.2890	580.41	4.7385	540.50
3.8290	613.59	4.6825	581.48	5.0234	541.63
4.1935	614.26	5.0946	582.53	5.3212	542.86
4.5428	614.93	5.5248	583.59	5.6140	543.95
4.9054	615.61	5.9722	584.68	5.9389	545.10
5.2637	616.27	6.4310	585.75	6.2684	546.35
5.6341	616.94	6.9233	586.94	6.6221	547.76
6.0113	617.61	7.4335	588.03	6.9786	548.98
6.3953	618.28	7.9350	589.22	7.3620	550.27
6.7886	618.96	8.4599	590.39	7.7365	551.56
7.1654	619.61	9.0240	591.62	8.1262	552.91
7.5581	620.28	9.5585	592.78	8.5255	554.11
7.9601	620.96			8.9798	555.58
8.3772	621.66			9.4880	557.04
8.7855	622.34			9.9898	558.59
9.2342	623.05				
9.6821	623.79				

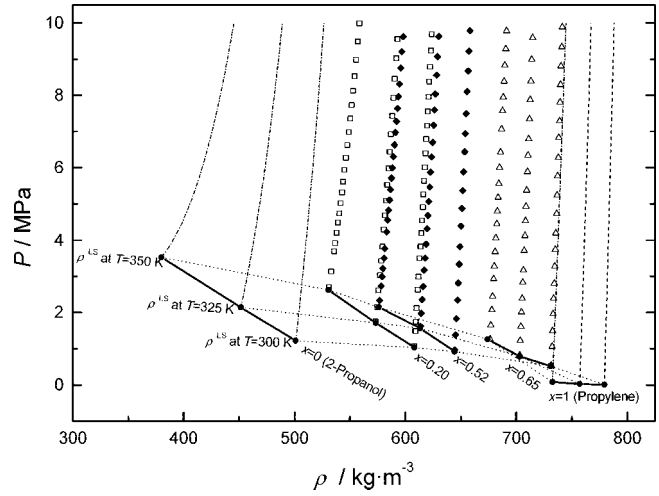

Figure 2. Liquid density measurements for the propylene (1) + 2-propanol (2) mixture.

the pressure, the temperature inside the VTD, and the period of vibration are recorded every 3 s. The period of vibration is converted into density using the Forced Path Mechanical Calibration (FPMC) method.[8] The first reference for the calibration is the period of vibration measured at vacuum conditions, while the second reference is with the refrigerant R134a, for which measurements have been carried out at the same temperature and in the same pressure range of the target mixture (see ref 8).

2.4. Experimental Uncertainties. The experimental uncertainties have been calculated taking into account the expanded uncertainties and coverage factor as described in ref 9. The global uncertainty on density data in the liquid phase is estimated to be within 0.05 %. The uncertainty on vibrating period values is $\pm 10^{-8}$ s. Global temperature uncertainties are estimated to be about $\pm$ 0.02 K with a confidence level of approximately 68 %. Global uncertainties on pressure measurement are $\pm$ 0.0001 MPa (for $(0 < P \leq 0.6)$ MPa) and $\pm$ 0.0006 MPa (for $(0.6 < P \leq 10.6)$ MPa) with a confidence level of approximately 68 %. Uncertainties in mixture composition are within $2 \cdot 10^{-4}$ in molar fraction.

3. Experimental Results

3.1. Liquid Density Results. The liquid density measurements for the propylene (1) + 2-propanol (2) mixture have been carried out at (300, 325, and 350) K from 10 MPa down to bubble pressures for the $x_1 =$ (0.20, 0.52, and 0.65) molar fractions. The measured (P, ρ, T) values are reported in Table 1. In Figure 2, the measured data are shown together with liquid density values of the pure propylene[10] and 2-propanol[11] at the same temperatures of the mixture measurements and for pressures from the pure fluid bubble points up to 10 MPa. Temperature dependence at constant composition of the propylene (1) + 2-propanol (2) mixture is shown in Figure 3a, while composition dependence at constant temperature is shown in Figure 3b.

3.2. Equilibrium Results. The VTD allows us to obtain density measurements, and furthermore, through a data reduction of such values, bubble pressures can also be evaluated as discussed in ref 6. In this way, bubble pressures for the propylene (1) + 2-propanol (2) mixture have been obtained at (300, 325, and 350) K for $x_1 =$ (0.20, 0.52, and 0.65) molar fractions. The values are reported in Table 2, while the Figure 4 shows the obtained values in comparison to the available literature data in the same temperature range.[2–4]

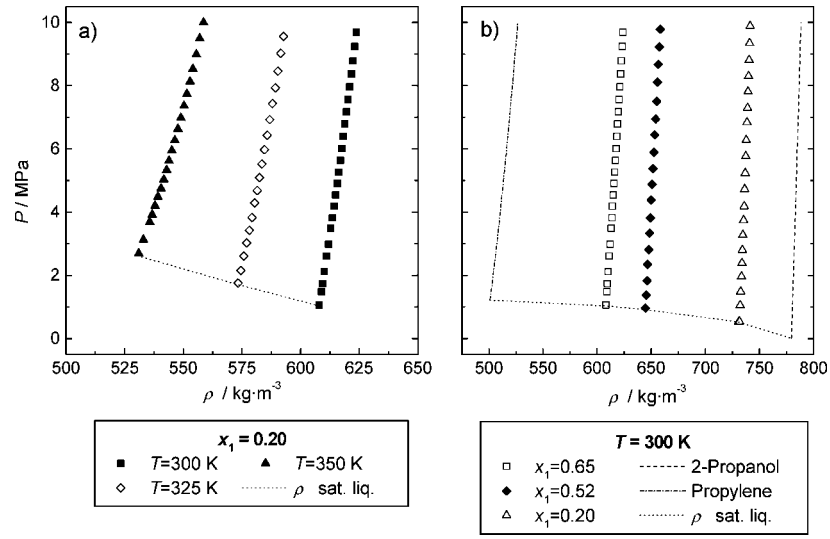

Figure 3. Propylene (1) + 2-propanol (2) mixture: (a) temperature dependence of the liquid density at constant composition ($x_1 = 0.20$); (b) composition dependence of the liquid density at constant temperature ($T = 300$ K).

Table 2. Comparison of Pressures and Densities at Bubble Point Conditions between Those Determined by the VTD (P and ρ) and Those by the Intersection of the Compressed Liquid Density MLFN Model and the Bubble Pressure MLFN Model (P' and ρ')

T	x_1	P	P'	ΔP	ρ	ρ'	$\Delta\rho$
K	(molar)	MPa	MPa	%	kg·m^{-3}	kg·m^{-3}	%
300.14	0.2011	0.5224	0.4956	−5.125	731.63	731.23	−0.055
300.11	0.5201	0.9192	0.9199	0.076	644.42	644.63	0.032
300.12	0.6478	1.0297	1.0021	−2.677	607.97	607.84	−0.022
325.09	0.2011	0.7850	0.8604	9.606	703.01	703.25	0.034
325.05	0.5201	1.5583	1.5658	0.481	613.29	613.39	0.017
325.13	0.6478	1.7095	1.7394	1.748	573.24	573.50	0.045
350.18	0.2011	1.2620	1.2840	1.743	676.38	676.63	0.037
350.12	0.5201	2.1521	2.3275	8.149	575.99	576.57	0.102
350.18	0.6478	2.6200	2.6342	0.542	530.66	530.79	0.025

4. Modeling Methods

Multilayer feedforward neural network (MLFN) functional forms have been used to correlate liquid density and bubble pressure experimental values. The general architecture of a MLFN is illustrated in Figure 5: it is composed of a certain number of units, called *neurons*, organized in three layers called the *input*, *hidden*, and *output* layers, respectively. The neurons of the input layer are indicated as elements of an array $\bar{U}$ of dimension I. Their number coincides with the number of independent variables of the equation plus one. The last neuron, labeled *Bias* 1, has a constant value

$$U_I = Bias\ 1 \tag{1}$$

The number of neurons of the output layer equals the output quantities, which are elements of an array $\bar{S}$ of dimension K.

The hidden layer performs the transformation of the signals from the input layer to the output layer, and it can contain an arbitrary number of neurons. These are elements of an array $\bar{H}$ of dimension $J + 1$. Also in the hidden layer, there is a bias neuron with a constant value, *Bias* 2

$$H_{J+1} = Bias\ 2 \tag{2}$$

The physical input variables V_i (temperature, pressure, and mole fraction for the liquid density correlation and temperature

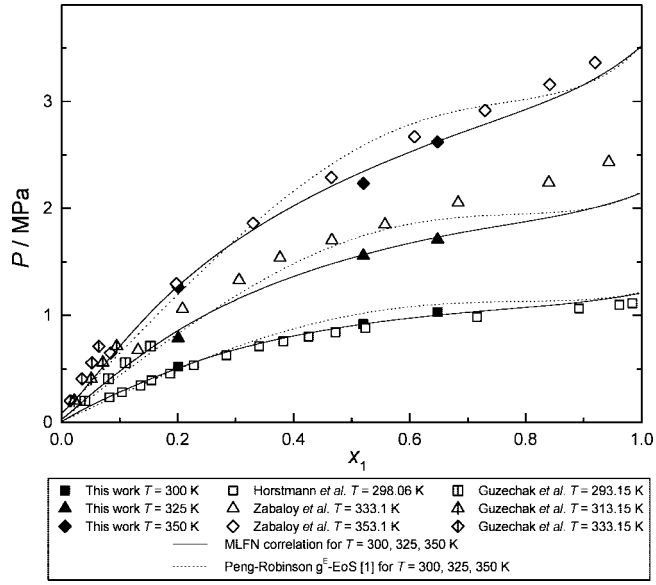

Figure 4. Bubble pressure data for the propylene (1) + 2-propanol (2) mixture.

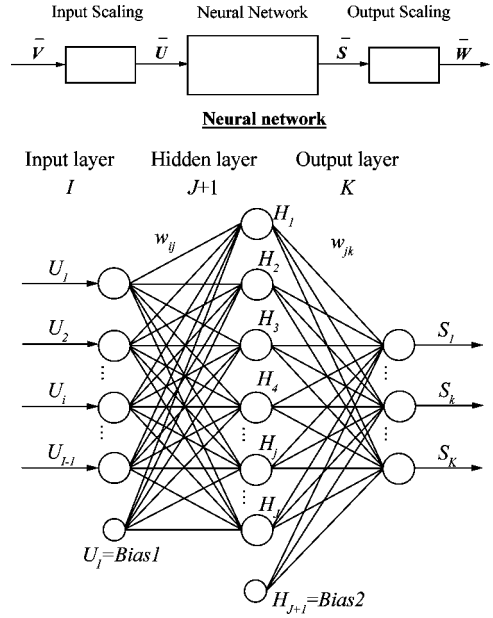

Figure 5. General topology of a three-layer feedforward neural network.

Table 3. Parameters of the Feedforward Neural Network Used for the Correlation of the Liquid Density Data for the Mixture Propylene (1) + 2-Propanol (2)

$\beta = 0.5$			$V_{min,1} = T_{min} = 250$			$V_{max,1} = T_{max} = 400$		
$I = 4$			$V_{min,2} = P_{min} = 0$			$V_{max,2} = P_{max} = 12$		
$J = 12$			$V_{min,3} = x_{min} = 0$			$V_{max,3} = x_{max} = 1$		
$K = 1$			$W_{min,1} = \rho_{min} = 350$			$W_{max,1} = \rho_{max} = 800$		
i	j	w_{ij}	i	j	w_{ij}	j	k	w_{jk}
1	1	$9.010170 \cdot 10^{1}$	3	1	$1.119710 \cdot 10^{2}$	1	1	$-4.617640 \cdot 10^{1}$
1	2	−7.888430	3	2	−9.451570	2	1	$1.045780 \cdot 10^{2}$
1	3	4.093740	3	3	$4.741180 \cdot 10^{1}$	3	1	$2.705210 \cdot 10^{1}$
1	4	$3.175850 \cdot 10^{1}$	3	4	$3.745950 \cdot 10^{1}$	4	1	$-3.218450 \cdot 10^{1}$
1	5	5.408060	3	5	4.226020	5	1	$4.131650 \cdot 10^{1}$
1	6	$1.160290 \cdot 10^{1}$	3	6	$6.257430 \cdot 10^{1}$	6	1	1.148660
1	7	−1.719460	3	7	$-6.859890 \cdot 10^{1}$	7	1	$7.869950 \cdot 10^{1}$
1	8	$2.384800 \cdot 10^{1}$	3	8	$3.126750 \cdot 10^{1}$	8	1	$7.177710 \cdot 10^{1}$
1	9	$-1.635840 \cdot 10^{2}$	3	9	$-5.275310 \cdot 10^{1}$	9	1	$-1.563460 \cdot 10^{2}$
1	10	$7.722330 \cdot 10^{2}$	3	10	$2.476070 \cdot 10^{2}$	10	1	$-7.446350 \cdot 10^{2}$
1	11	9.913330	3	11	8.709160	11	1	$-8.324710 \cdot 10^{1}$
1	12	$2.627740 \cdot 10^{-1}$	3	12	$-9.278200 \cdot 10^{1}$	12	1	$-7.044190 \cdot 10^{1}$
2	1	$-3.232040 \cdot 10^{1}$	4	1	$-1.615050 \cdot 10^{2}$	13	1	$3.140790 \cdot 10^{1}$
2	2	$-6.101320 \cdot 10^{-2}$	4	2	$2.656600 \cdot 10^{1}$			
2	3	$9.660710 \cdot 10^{-4}$	4	3	$1.236170 \cdot 10^{2}$			
2	4	$-4.646080 \cdot 10^{1}$	4	4	$6.156810 \cdot 10^{1}$			
2	5	$-5.914600 \cdot 10^{-1}$	4	5	$-4.362300 \cdot 10^{-1}$			
2	6	−7.413220	4	6	$-6.507460 \cdot 10^{1}$			
2	7	1.424330	4	7	−1.663850			
2	8	$2.367740 \cdot 10^{1}$	4	8	$3.043150 \cdot 10^{1}$			
2	9	$9.005100 \cdot 10^{1}$	4	9	$1.339450 \cdot 10^{2}$			
2	10	$-4.175130 \cdot 10^{2}$	4	10	$-6.333350 \cdot 10^{2}$			
2	11	$-7.045390 \cdot 10^{-1}$	4	11	$-9.259080 \cdot 10^{-1}$			
2	12	1.699010	4	12	−2.553360			

Table 4. Accuracy of the Feedforward Neural Network Model in the Representation of the Liquid Density Data of the Propylene (1) + 2-Propanol (2) Mixture

system	ref	NPT[a]	T range (K)	P range (MPa)	x_1 range	AAD (%)	Bias (%)	MAD (%)
binary mixture	this work	186	300.0 to 350.2	0.0 to 10.1	0.20 to 0.65	0.017	0.006	0.063
2-propanol	Stringari et al.[11]	123	300.0 to 350.0	0.0 to 10.0	0.00	0.019	0.008	0.035
propylene	Angus et al. (DEoS)[10]	98	300.0 to 350.0	1.2 to 10.1	1.00	0.028	0.014	0.099
		407	300.0 to 350.2	0.0 to 10.1	0.00 to 1.00	0.020	0.009	0.099

[a] NPT: number of experimental points.

and composition for the bubble pressure correlation) undergo a linear transformation to normalize them in the arbitrarily chosen range $[A_{min}, A_{max}]$ set as $A_{min} = 0.05$ and $A_{max} = 0.95$

$$U_i = u_i(V_i - V_{i,min}) + A_{min} \quad \text{for} \quad 1 \le i \le I - 1 \tag{3}$$

where

$$u_i = \frac{A_{max} - A_{min}}{V_{i,max} - V_{i,min}} \tag{4}$$

and $V_{i,min}$ and $V_{i,max}$ represent the selected extremes of the range of the variable V_i. An arctangent function normalized in the range [0,1] is assumed as the transfer function

$$g(z) = \frac{1}{\pi}\arctan(\beta \cdot z) + 0.5 \tag{5}$$

The transfer function calculates the signal output of a neuron from its inputs for both the hidden and the output layer neurons; respectively, it is

$$H_j = g\left(\sum_{i=1}^{I} w_{ij}U_i\right) \quad \text{for} \quad 1 \le j \le J \tag{6}$$

$$S_k = g\left(\sum_{j=1}^{J+1} w_{ijk}U_j\right) \quad \text{for} \quad 1 \le k \le K \tag{7}$$

The symbols w_{ij} and w_{jk} indicate the *weighting factors* that are the free parameters of the model, which must be determined in the regression process. The output values S_k of the output layer neurons are denormalized to real output variables W_k,

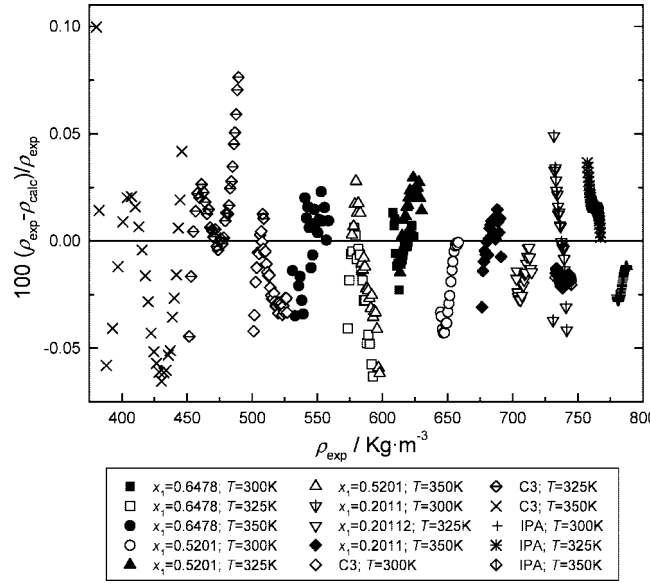

Figure 6. Percentage error of the feedforward neural network model in the representation of the liquid density data of the propylene (1) + 2-propanol (2) mixture: C3 = propylene, IPA = 2-propanol.

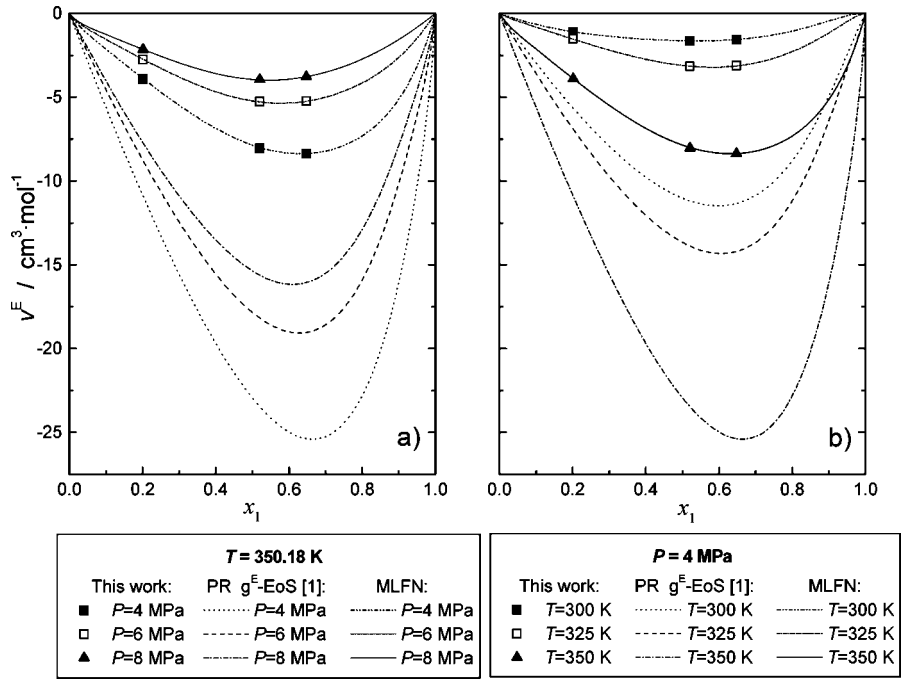

Figure 7. Excess molar volumes for the propylene (1) + 2-propanol (2) mixture: (a) pressure dependence at constant temperature; (b) temperature dependence at constant pressure.

which are in this case either density or bubble pressure, through the following linear transformation

$$W_k = \frac{S_k - A_{\min}}{s_k} + W_{k,\min} \quad \text{for} \quad 1 \le k \le K \tag{8}$$

where

$$s_k = \frac{A_{\max} - A_{\min}}{W_{k,\max} - W_{k,\min}} \tag{9}$$

$W_{k,\min}$ and $W_{k,\max}$ are the chosen limits of the range of the dependent variable W_k.

5. Discussion

The measured values of liquid density and bubble pressure for the propylene (1) + 2-propanol mixture have been represented with MLFN functions presented in the previous section, and a statistical analysis of the data representation is reported in the following.

In such a context, the error deviation ΔM_i of the ith point of a property M, the percentage average absolute deviation AAD %, the Bias %, and the percentage maximum absolute deviation MAD % with respect to a database of NPT values are evaluated as

$$\Delta M_i = \left(\frac{M_{\text{calcd}} - M_{\text{exptl}}}{M_{\text{exptl}}}\right)_i \tag{10}$$

$$\text{AAD \%} = 100 \cdot \frac{1}{\text{NPT}} \sum_{i=1}^{\text{NPT}} |\Delta M_i| \tag{11}$$

$$\text{Bias \%} = 100 \cdot \frac{1}{\text{NPT}} \sum_{i=1}^{\text{NPT}} \Delta M_i \tag{12}$$

$$\text{MAD \%} = 100 \cdot \max_{i=1,\text{NPT}} |\Delta M_i| \tag{13}$$

M represents here the liquid density ρ or the bubble pressure p^{bub}.

The measured liquid density values, together with the liquid density values of pure propylene[10] and of pure 2-propanol,[11] at the same temperatures of the mixture measurements and for pressures ranging from the pure fluid bubble points up to 10 MPa, were correlated with a MLFN. The parameters used for the correlation of the liquid density data are presented in Table 3. Residual errors are presented in Table 4 and shown graphically in Figure 6. The simultaneous representation of mixture and pure fluid data shows a good coherence among the measured liquid density values for the mixture and independent density values for the pure fluids.

Using the obtained MLFN function, excess molar volumes have been calculated, and their composition dependence has been shown, varying pressure at constant temperature, in Figure 7a, and varying temperature at constant pressure, in Figure 7b. In the same figures, also the excess molar volumes calculated with the Peng–Robinson EoS including the Wong−Sandler mixing rules as obtained for this system in ref 1 have been shown for comparison. A very good agreement between experimental excess volume values and values predicted by the MLFN can be noted in Figure 7. This result comes from the very low residual error (AAD % = 0.0201) in the representation of the pure fluids and mixture density values with the MLFN. On the other hand the Peng–Robinson EoS[1] represents the excess molar volumes only in a qualitative way, confirming that such an EoS is not precise enough in the representation of compressed liquid densities, especially for systems involving associating fluids.

The coefficients of a second MLFN have been regressed on the literature bubble pressure values[2,4] and on the saturation pressure of the pure propylene[10] and pure 2-propanol.[12] The parameters used for the correlation of the bubble pressure data are presented in Table 5. The percentage errors of the obtained MLFN with respect to the measured bubble pressures are presented in Table 6 together with the errors with respect to the literature data available in the same range of temperatures. The AAD % with respect to the measured values is greater

Table 5. Parameters of the Feedforward Neural Network Used for the Correlation of the Bubble Pressure Data for the Mixture Propylene (1) + 2-Propanol (2)

$\beta = 0.5$			$V_{min,1} = T_{min} = 250$			$V_{max,1} = T_{max} = 400$		
$I = 3$			$V_{min,2} = x_{min} = 0$			$V_{max,3} = x_{max} = 1$		
$J = 10$			$W_{min,2} = P_{min}^{bub} = 0$			$W_{max,1} = P_{max}^{bub} = 12$		
$K = 1$								
i	j	w_{ij}	i	j	w_{ij}	j	k	w_{jk}
1	1	−2.984260	2	6	−8.020910	1	1	$-4.286830 \cdot 10^{1}$
1	2	−2.368580	2	7	$-1.477240 \cdot 10^{1}$	2	1	$1.003870 \cdot 10^{1}$
1	3	$-5.797060 \cdot 10^{-2}$	2	8	1.219770	3	1	$-1.594220 \cdot 10^{1}$
1	4	−7.176010	2	9	$6.848890 \cdot 10^{1}$	4	1	$1.780930 \cdot 10^{1}$
1	5	8.495830	2	10	2.736060	5	1	$-3.840020 \cdot 10^{1}$
1	6	5.252270	3	1	2.109340	6	1	6.209550
1	7	−6.099100	3	2	5.568850	7	1	$-3.350460 \cdot 10^{1}$
1	8	−1.445960	3	3	$9.371590 \cdot 10^{-1}$	8	1	$5.234110 \cdot 10^{1}$
1	9	$-3.605730 \cdot 10^{1}$	3	4	4.846480	9	1	$5.640040 \cdot 10^{-1}$
1	10	9.521860	3	5	−4.758900	10	1	$2.152770 \cdot 10^{1}$
2	1	$-1.685540 \cdot 10^{-1}$	3	6	−4.523590	11	1	5.090110
2	2	−5.177630	3	7	4.351610			
2	3	$-3.103680 \cdot 10^{1}$	3	8	$5.681530 \cdot 10^{-2}$			
2	4	−4.547720	3	9	$-5.409480 \cdot 10^{1}$			
2	5	$1.348860 \cdot 10^{1}$	3	10	−4.652040			

Table 6. Accuracy of the Feedforward Neural Network Model in the Representation of the Bubble Pressure Data of the Propylene (1) + 2-Propanol (2) Mixture

ref	NPT	T range (K)	P range (MPa)	x_1 range	AAD (%)	Bias (%)	MAD (%)
this work	9	300.1 to 350.2	0.5 to 2.6	0.20 to 0.65	3.350	1.616	9.606
Horstmann et al.[4]	17	298.1	0.2 to 1.1	0.08 to 1.00	0.506	0.191	2.594
Zabaloy et al.[2]	17	333.1 to 353.1	0.6 to 3.4	0.08 to 0.94	0.794	–0.037	2.223
Guzechak et al.[3]	12	293.2 to 333.2	0.2 to 0.7	0.02 to 0.15	50.999	–50.999	59.794
	55	300.1 to 353.1	0.2 to 3.4	0.02 to 1.00	12.077	–10.815	59.794

than the AAD % with respect to the literature data on which the weighting factors of the MLFN have been regressed. The AAD of the measured bubble pressures is about 3.35 %, while a value significantly lower is found for the literature data of refs 2 and 4. At the same time, it can be noted that literature data from ref 3 are not at all consistent with all the other bubble pressure data. A comparison between the MLFN predictions and the measured bubble pressures is shown in Figure 4. In the same figure, the bubble pressures predicted by the MLFN are compared with the Peng–Robinson EoS using Wong−Sandler mixing rules, whose parameters were presented in ref 1.

From the intersection of the MLFN function regressed on single phase liquid densities and the MLFN function regressed on bubble pressures, it is possible to obtain an accurate representation of the saturated liquid density surface of the mixture as a function of temperature and composition. Figure 8 shows several isothermal sections of such a surface pointing out the regular trends in the saturated liquid density representation by the developed model. Using the same approach, the saturated liquid densities at the present experimental temperature and composition values have been calculated, and the results are reported in Table 2 as ρ'. In the same table, the bubble pressures calculated by the MLFN model P' are also reported for comparison. The percentage relative deviation among the two evaluation methods of the saturated liquid density is quite close to the experimental uncertainty of the density measurements. The percentage deviations among the bubble pressures determined from the experimental data through the graphical procedure and the corresponding ones generated by the MLFN model are also reported in the table. Reference is also made to former Table 6 and its relative comments.

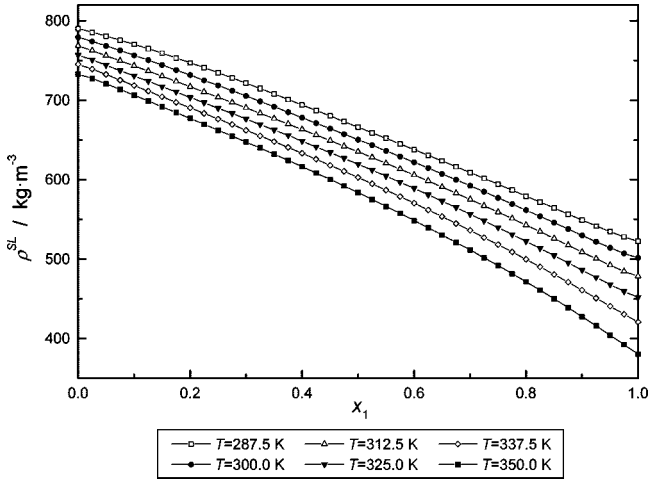

Figure 8. Saturated liquid density prediction for the propylene (1) + 2-propanol (2) mixture obtained as intersection of the feedforward neural network correlations for the liquid densities and for the bubble pressures.

6. Conclusions

Liquid densities for the propylene (1) + 2-propanol (2) mixture have been measured at (300, 325, and 350) K from 10 MPa down to bubble pressures and $x_1 =$ (0.20, 0.52, and 0.65) molar fractions. The measured liquid density values have been correlated with a MLFN including liquid density values of the pure components, showing a good consistency of the mixture measurements with the pure fluid data. Excess molar volumes have been calculated, and their trend is consistent with the Peng–Robinson EoS using Wong−Sandler mixing rules.

Bubble pressures for the propylene (1) + 2-propanol (2) mixture have been obtained at (300, 325, and 350) K and $x_1 =$ (0.20, 0.52, and 0.65) molar fractions. The measured values have been compared with a MLFN function with coefficients

regressed on literature data in the same range of temperatures of the measurements carried out in this work.

The saturated liquid density surface in the temperature and pressure range of the measurements presented in this work has been obtained as an intersection of the MLFN function regressed on single-phase liquid densities and the MLFN function regressed on bubble pressures.

Literature Cited

(1) Grigiante, M.; Stringari, P.; Scalabrin, G.; Ihmels, C.; Fischer, K.; Gmehling, J. Vapor−liquid−liquid equilibria and excess molar enthalpies of binary and ternary mixtures of 2-propanol, water, and propylene. *J. Chem. Thermodyn.* **2007,** doi: 10.1016/j.jct.2007.12.002.

(2) Zabaloy, M.; Mabe, G.; Bottini, S. B.; Brignole, E. A. Isothermal vapor−liquid equilibrium data for the binaries propane-2-propanol and propylene-2-propanol. *J. Chem. Eng. Data* **1993**, *38*, 40–43.

(3) Guzechak, O. Y.; Sarancha, V. N.; Romanyuk, I. M.; Yavorskaya, O. M.; Churik, G. P. Solubility of propylene in organic solvents. *J. Appl. Chem. USSR* **1984**, *57*, 1663–1665.

(4) Horstmann, S.; Gardeler, H.; Bölts, R.; Rarey, J.; Gmehling, J. Isothermal Vapor−Liquid Equilibrium and Excess Enthalpy Data for the Binary Systems Diethyl Ether + Ethyl *tert*-Butyl Ether, 1-Pentene + Methyl Acetate, and Propene + 2-Propanol. *J. Chem. Eng. Data* **1999**, *44*, 383–387.

(5) Khalil, W.; Coquelet, C.; Richon, D. High-Pressure Vapor−Liquid Equilibria, Liquid Densities, and Excess Molar Volumes for the Carbon Dioxide + 2-Propanol System from (308.10 to 348.00) K. *J. Chem. Eng. Data* **2007**, *52*, 2032–2040.

(6) Bouchot, C.; Richon, D. Direct Pressure−Volume−Temperature and Vapor−Liquid Equilibrium Measurements with a Single Equipment Using a Vibrating Tube Densimeter up to 393 K and 40 MPa: Description of the Original Apparatus and New Data. *Ind. Eng. Chem. Res.* **1998**, *37*, 3295–3304.

(7) Galicia-Luna, L. A.; Richon, D.; Renon, H. New Loading Technique for a Vibrating Tube Densimeter and Measurements of Liquid Densities up to 39.5 MPa for Binary and Ternary Mixtures of the Carbon Dioxide−Methanol−Propane System. *J. Chem. Eng. Data* **1994**, *39*, 424–431.

(8) Bouchot, C.; Richon, D. An enhanced method to calibrate vibrating tube densimeters. *Fluid Phase Equilib.* **2001**, *191*, 189–208.

(9) Taylor, B. N.; Kuyatt, C. E. *NIST Technical Note 1297*, National Institute of Standards and Technology: Gaithersburg, MD, 1994 (see also at: http://physics.nist.gov/cuu/Uncertainty/index.html).

(10) Angus, S.; Armstrong, B.; de Reuck, K. M., *International Thermodynamic Tables of the Fluid State-7 Propylene, International Union of Pure and Applied Chemistry*; Pergamon Press: Oxford, 1980.

(11) Stringari, P.; Scalabrin, G.; Richon, D. Density measurements of 2-propanol in the liquid region. **2008**, submitted for publication.

(12) Poling, B. E. Vapor pressure prediction and correlation from the triple point to the critical point. *Fluid Phase Equilib.* **1996**, *116*, 102–109.

Received for review January 7, 2008. Accepted February 1, 2008. P. Stringari is grateful to Fondazione Ing. Aldo Gini (Padova, Italy) for financial support.

JE800017J